

RESEARCH ARTICLE



Berberine regulates the Notch1/PTEN/PI3K/AKT/mTOR pathway and acts synergistically with 17-AAG and SAHA in SW480 colon cancer cells

Ge Li^a, Chuang Zhang^b, Wei Liang^a, Yanbing Zhang^b, Yunheng Shen^c and Xinhui Tian^a

^aInstitute of Interdisciplinary Integrative Medicine Research, Shanghai University of Traditional Chinese Medicine, Shanghai, PR China;

^bSchool of Pharmacy, Zhengzhou University, Zhengzhou, PR China; ^cSchool of Pharmacy, Naval Medical University, Shanghai, PR China

ABSTRACT

Context: Berberine (BBR) is used to treat diarrhoea and gastroenteritis in the clinic. It was found to have anticolon cancer effects.

Objective: To study the anticolon cancer mechanism of BBR by connectivity map (CMAP) analysis.

Materials and methods: CMAP based mechanistic prediction was conducted by comparing gene expression profiles of 10 μ M BBR treated MCF-7 cells with that of clinical drugs such as helveticoside, ianatoside C, pyrinium, gossypol and trifluoperazine. The treatment time was 12 h and two biological replications were performed. The DMSO-treated cells were selected as a control. The interaction between 100 μ M BBR and target protein was measured by cellular thermal shift assay. The protein expression of 1–9 μ M BBR treated SW480 cells were measured by WB assay. Apoptosis, cell cycle arrest, mitochondrial membrane potential (MMP) of 1–9 μ M BBR treated SW480 cells were measured by flow cytometry and Hoechst 33342 staining methods.

Results: CMAP analysis found 14 Hsp90, HDAC, PI3K or mTOR protein inhibitors have similar functions with BBR. The experiments showed that BBR inhibited SW480 cells proliferation with IC_{50} of 3.436 μ M, induced apoptosis, autophagy, MMP depolarization and arrested G1 phase of cell cycle at 1.0 μ M. BBR dose-dependently up-regulated PTEN, while inhibited Notch1, PI3K, Akt and mTOR proteins at 1.0–9.0 μ M ($p < 0.05$). BBR also acted synergistically with Hsp90 and HDAC inhibitor (0.01 μ M) in SW480 cells at 0.5 and 1.0 μ M.

Discussion and conclusions: The integrative gene expression-based chemical genomic method using CMAP analysis may be applicable for mechanistic studies of other multi-targets drugs.

ARTICLE HISTORY

Received 3 April 2020

Revised 2 November 2020

Accepted 10 December 2020

KEYWORDS



Connectivity map;
synergistic
effect; mechanism

Introduction

Natural products and their derivatives account for 37.3% of approved antitumor drugs due to chemical structure diversity, better biocompatibility and drug-like properties (Newman and Cragg 2016). Berberine (BBR) is a natural product first isolated from the bark of *Zanthoxylon clava herculis* Linne (Rutaceae) in 1826, it is used clinically for diarrhoea and gastroenteritis. BBR was reported to have a variety of other pharmacological effects such as antitumor (Farooqi et al. 2019; Gao et al. 2019; Mohammadinejad et al. 2019; Yao et al. 2019), antidiabetic and hypolipidemic (Lan et al. 2015; Sahebkar and Watts 2017; Ma et al. 2018), diminishing liver fibrosis (Feng et al. 2009), neuro-protective (Pirmoradi et al. 2019), anti-inflammatory (Lu et al. 2019) and antioxidant (Kazaz et al. 2020). Colon cancer, the third most prevalent cancer worldwide, is increasing in individuals less than 50 years old (Siegel et al. 2019). The common treatments of colon cancer include surgery, radiotherapy, chemotherapy and molecular targeted therapy. Despite the great improvements in diagnostic and therapeutic methods, the prognosis of colon cancer remains poor. Therefore, investigation of novel drugs as well as the underlying molecular mechanisms is very necessary. Recently, intensive studies have found that BBR

exerts anticolon cancer effect by interacting with AMPK (Park et al. 2012; Li et al. 2015), TGF- β (Huang, Tao et al. 2019, Huang, Wang et al. 2019), EGFR (Wang et al. 2013), ROS (Hsu et al. 2007; Wang et al. 2012), Wnt/ β -catenin (Wu et al. 2012; Ruan et al. 2017), microRNAs (Huang et al. 2017; Lü et al. 2018), inflammation (Fukuda et al. 1999; Chidambara Murthy et al. 2012; Xu et al. 2012), arylamine *N*-acetyltransferase (Lin et al. 1999), glucose metabolism (Mao et al. 2018), Cl^- secretion (Alzamora et al. 2011) and intestinal mucosal permeability (Wu et al. 2018). The above studies indicated the significant application potential of BBR in colon cancer treatment. However, does BBR act on other unknown targets or pathways? Can it be used in combination with other clinical anticancer drugs? We innovatively apply CMAP analysis to study the anticolon cancer mechanism of BBR and obtain novel information.

The connectivity map (CMAP) is a database constructed of more than 7000 gene expression profiles of drug treated cells which can identify the connection between drugs, diseases and genes (Lamb et al. 2006). By comparing the gene expression profiles of the compound with that of 1309 FDA-approved drugs, we can quickly discover the targets of our compounds, elucidate the possible mechanisms, and find new uses of clinical drugs (Hieronymus et al. 2006; Lv et al. 2017, 2018). In this study,

CONTACT Xinhui Tian  tianxinhui@126.com  Institute of Interdisciplinary Integrative Medicine Research, Shanghai University of Traditional Chinese Medicine, Shanghai, PR China

© 2021 The Author(s). Published by Informa UK Limited, trading as Taylor & Francis Group.

This is an Open Access article distributed under the terms of the Creative Commons Attribution License (<http://creativecommons.org/licenses/by/4.0/>), which permits unrestricted use, distribution, and reproduction in any medium, provided the original work is properly cited.

CMP database (<http://www.broadinstitute.org/cmap/>) was applied to identify potential anticolon cancer mechanism of BBR.

Materials and methods

Cells, reagents and antibodies

The human colon cancer cells SW480, the human hepatoma cancer cells HuH7, QGY7701 and QGY7703, the human breast cancer cells MCF-7, the human lung cancer cells A549 and the human acute monocytic leukaemia cells THP-1 were obtained from the Cell Resource Centre, Institute of Life Sciences, Chinese Academy of Medical Science. Berberine (>98% pure) was purchased from Sigma-Aldrich (St. Louis, MO). Tanespimycin (17-AAG) and Vorinostat (SAHA) were from Medchem Express (Monmouth Junction, NJ). L-15 medium, DMEM medium and penicillin/streptomycin were from Gibco (Carlsbad, CA). Foetal bovine serum was from Biological Industries (Cromwell, CT). Hoechst 33342 dye was from Sigma-Aldrich Corp. (St. Louis, MO). Annexin V-FITC was from BD Biosciences (San Jose, CA). Cell Cycle and Apoptosis Analysis Kit was from Beyotime (Nantong, China). Protease inhibitor cocktail and BCA protein quantitation kit were from Thermo Fisher (Rockford, IL).

Antibodies specific for β -actin (#4970), Hsp70 (#4872), IKK β (#2678), EGFR (#4267), phospho-PI3K (#4228), PI3K (#4257), phosphohospho-Akt (#4060), Akt (#9272), phosphohospho-mTOR (Ser2448) (#5536), phosphohospho-mTOR (Ser2481) (#2974), mTOR (#2983), CDK4 (#12790), cyclinD1 (#2978), LC3B (#3868), Bcl-2 (#2872), BAX (#5023), PARP (#9542), cleaved caspase-3 (#9661), cleaved caspase-9 (#9509), Jagged1 (#70109), Notch1 (#3608), NICD (#4147), Hes1 (#11988) and PTEN (#9188) were obtained from Cell Signaling Technology (Danvers, MA). Anti-Hsp90 (#ab13492) antibodies were from Abcam (Cambridge, UK). Antibodies specific for HDAC1 (sc-7872), HDAC2 (sc-7899), HDAC3 (sc-11417), HDAC4 (sc-11418), HDAC6 (sc-11420) and HDAC8 (sc-11405) were purchased from Santa Cruz Biotechnology (Dallas, TX).

CCK-8 assay

The cytotoxicity of BBR against cancer cells was assessed by using Cell Counting Kit-8. The assay was performed in triplicate. All cells were seeded in 96-well plate at a density of 5×10^3 cells/well at 37°C. After cell attachment overnight, each well was treated with different concentrations of BBR or 0.1% DMSO for 24 h, respectively. Then, 10 μ L of WST-8 solution was added to each well and the cultures were incubated for another 2 h. The absorbance was read at 450 nm by a SYNERGY microplate reader (Bio Tek, Winooski, VT) (Tian et al. 2016).

Hoechst 33342 staining

SW480 cells were first incubated with BBR for 24 h, then the cells were stained with Hoechst 33342 for 15 min in the dark. After washed by cold PBS, the cells were observed under the fluorescence microscope at 355/465 nm. Five randomly selected areas of each group were photographed (Mondal and Bennett 2016).

Annexin V-FITC/PI double-staining assay

The SW480 cells were seeded in six-well plates (3.5×10^5 cells/well) for 24 h and then treated with BBR for another 24 h. The cells were detached with 0.05% trypsin, washed three times with cold PBS, and centrifuged at 1500 rpm for 5 min at 4°C. Subsequently, SW480 cells were gently suspended in the binding buffer containing 5 μ L (10 μ g/mL) Annexin V-FITC for 15 min in the dark, then incubated with 10 μ L of PI (20 μ g/mL) for another 5 min. The cells were immediately analysed by flow cytometry (BD FACSCanto II) (Tian et al. 2016).

Determination of mitochondrial membrane potential (MMP)

The SW480 cells were treated with different concentrations of BBR for 24 h, and then incubated with 5 μ g/mL of rhodamine 123 for 30 min in the dark. After centrifuged at 1500 rpm for 5 min, and washed with cold PBS for three times, the cells were re-suspend in 1000 μ L of PBS and analysed by using flow cytometry at 488 and 530 nm, respectively (Tian et al. 2016).

Cell cycle analysis

SW480 cells were incubated with BBR for 24 h, and then trypsinized, washed with PBS, and fixed with 70% of ethanol at 4°C overnight. After washed twice with PBS, the cells were incubated with 100 μ L of RNase A for 30 min and then stained with 1 mL of PI for 10 min in the dark. The cell-cycle distribution was analysed by flow cytometry (Tian et al. 2016).

Cellular thermal shift assay (CETSA)

The SW480 cells (have been incubated with BBR for 30 min) were collected, washed three times with cold PBS, and then lysed in PBS supplemented with protease inhibitors following three cycles of freeze-thaw. Cell lysates were then centrifuged at 13,000 rpm for 15 min, the supernatant was diluted with cold PBS and divided into two equal parts, with one part treated with DMSO and the other part treated with BBR (100 μ M). After incubation at room temperature for 30 min, the two parts were divided into nine aliquots (60 μ L) respectively, then heated at temperatures of 40, 44, 48, 52, 56, 60, 64, 68 and 72°C for 3 min. The samples were cooled for 3 min at room temperature and kept on ice. Then, every aliquot was centrifuged and the supernate was analysed by Western blot (Lv et al. 2018).

Western blot analysis

The SW480 cells (the interaction time of drugs and cells was 24 h) were lysed with the ice-cold RIPA buffer containing 1% protease inhibitor cocktail for 15 min and then centrifuged. Total protein concentrations of the lysates were assessed using BCA protein quantitation kit. Protein samples were separated by SDS-polyacrylamide gel electrophoresis in 6–12% gels and then transferred onto methanol activated PVDF membranes at 220 mA. The PVDF membranes were blocked with 5% skim milk for 20 min, probed with the indicated primary antibody and blotted with the secondary antibody for 1 h at room temperature. Object proteins were detected by Bio-Rad ChemiDoc™ (Hercules, CA) (Lv et al. 2018).

Results

BBR inhibits proliferation and induces apoptosis of SW480 cells

We found that colon cancer cells SW480 were more sensitive to BBR treatment with IC_{50} of $3.43\ \mu\text{M}$ when compared with human colon cancer cells HCT116, human breast adenocarcinoma cells MCF-7, human hepatocellular carcinoma cells QGY-7703, QGY-7701, HuH-7, human monocytic leukaemia cells THP-1 and human non-small-cell lung carcinoma cells A549 (Table 1). Further studies showed that BBR can attenuate SW480 cells proliferation in a time and dose-dependent manner at 0.5, 1, 2, 4, and $8\ \mu\text{M}$ (Figure 1).

Apoptosis is considered to be one of the main mechanisms to prevent the development of cancer. Thus, BBR-induced SW480 cells apoptosis was investigated by using Hoechst 33342 staining method. The blank group showed a uniformly dispersed light blue, while the BBR treated cells showed a blocky bright blue in the staining area, which is a sign of chromatin condensation. The chromatin condensation is one of the hallmarks of apoptosis. Thus, the Hoechst 33342 staining results indicated that BBR induced the apoptosis of SW480 cells at concentrations of $1\text{--}9\ \mu\text{M}$ (Figure 2(A)).

Annexin V-FITC/PI double staining method was used to further study BBR-induced apoptosis in SW480 cells. The right upper and lower right quadrants of the figure represented late and early stages of cells apoptosis. As shown in Figure 2(B,D), BBR induced early and late stages of apoptosis at $1\text{--}9\ \mu\text{M}$.

Table 1. Cytotoxicity effects of BBR on cancer cells ($IC_{50}\ \mu\text{M}$).

| Cells | BBR ^a | Doxorubicin ^{a,b} |
|----------|--------------------|----------------------------|
| MCF-7 | 36.277 ± 1.134 | 0.18 ± 0.004 |
| QGY-7701 | >100 | 0.17 ± 0.001 |
| QGY-7703 | >100 | 0.53 ± 0.010 |
| HuH7 | >100 | 0.79 ± 0.001 |
| THP-1 | 58.891 ± 2.732 | 0.04 ± 0.002 |
| A549 | >100 | 0.08 ± 0.001 |
| HCT116 | 44.736 ± 1.994 | 0.06 ± 0.004 |
| SW480 | 3.436 ± 0.193 | 0.14 ± 0.001 |

^a $n = 3$, means \pm S.D.

^bPositive control.

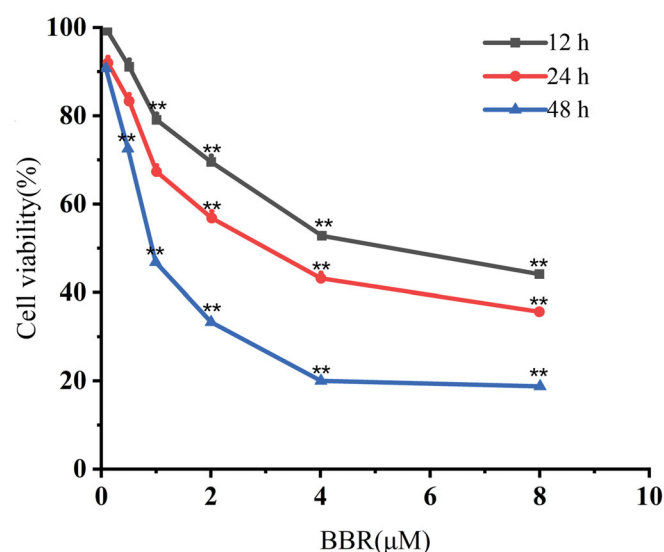


Figure 1. Cell viability of SW480 cells after exposure to $0\text{--}8\ \mu\text{M}$ of BBR for 12, 24 and 48 h, respectively. The results are expressed as the means of three independent experiments.

Depolarization of MMP is another characteristic of apoptosis. The decreased MMP in SW480 cells indicated that BBR-induced apoptosis was related with mitochondrial dysfunction (Figure 2(C,E)). Western blot analysis is then applied to detect whether BBR interfere with mitochondrial apoptotic pathway. First, Bcl-2 and Bax cause the mitochondrial membrane permeability changes, caspase-9 is cleaved and activated subsequently, then the apoptotic performer caspase-3 is activated, c-PARP is the cleavage substrate of caspase-3 which further regulates apoptosis. The exposure of $1\text{--}9\ \mu\text{M}$ BBR to SW480 cells resulted in the up-regulating of Bax, c-caspase-9, c-caspase-3 and c-PARP, and down-regulating of Bcl-2 (Figures 2(F) and 3(A)). The above results indicated that BBR induced apoptosis follows the mitochondrial pathway.

CMAP analysis predicts potential molecular mechanisms of BBR

Herein, CMAP was applied to identify the potential molecular mechanisms of BBR. The gene expression profiles of BBR treated cells are detected by microarray hybridization and scanning experiment using Affymetrix Human Genome U133A 2.0 chip, and a total of 526 up-regulated and 357 down-regulated genes (fold change ≥ 2) were obtained (Lv et al. 2017). These data were submitted into CMAP database (Version 2.0) for analysis and 14 drugs with lower p values and positive enrichment score were obtained (Table 2). Drugs with connectivity score closer to +1 act as higher similar to the interest, closer to -1 act as opposed to the interest, closer to 0 is unrelated to the interest. By analysing the targets of these obtained clinical drugs, we speculated that BBR may exert its antitumor activity by inhibiting Hsp90, HDAC, PI3K and mTOR proteins.

BBR did not interact with Hsp90 and HDACs in SW480 cells

The CMAP analysis revealed that BBR may be an Hsp90 inhibitor. The chaperone heat shock protein 90 (Hsp90) is responsible for the correct folding of both newly synthesized polypeptides and denatured proteins. It has hundreds of client proteins which involved in multiple oncogenic processes. Thus, Hsp90 is a promising tumour target (Neckers 2007; Schopf et al. 2017). The direct interaction between BBR and Hsp90 was examined by CETSA (Molina et al. 2013). Hsp90 protein expression decreased continuously as the incubation temperature increased. There was no significant difference between the control and BBR group, indicating that BBR did not interact directly with Hsp90 in SW480 cells (Figure 4(A,B)). Client proteins such as IKK and EGFR will be inhibited, while Hsp70 will be activated when Hsp90 is inhibited (Neckers 2007; Schopf et al. 2017). The indirect interaction between BBR and Hsp90 was then detected by analysing the above client proteins, and the results showed that BBR did not affect IKK, EGFR and Hsp70 when comparing with the positive control (Figure 4(C)). Therefore, BBR does not interact directly or indirectly with Hsp90 like a true Hsp90 inhibitor as CMAP predicted.

The CMAP analysis also revealed that BBR may function as a histone deacetylase (HDAC) inhibitor. HDAC can remove the acetyl group from histone, make the chromatin structure more compact, and silence tumour suppressor genes ultimately, thus inhibition of HDACs is considered a potential strategy for treating cancers (Xu et al. 2007). Western blot assay showed that protein levels of HDACs 1–4, 6, 8 in SW480 cells did not change as the concentrations of BBR increased, suggesting that BBR was

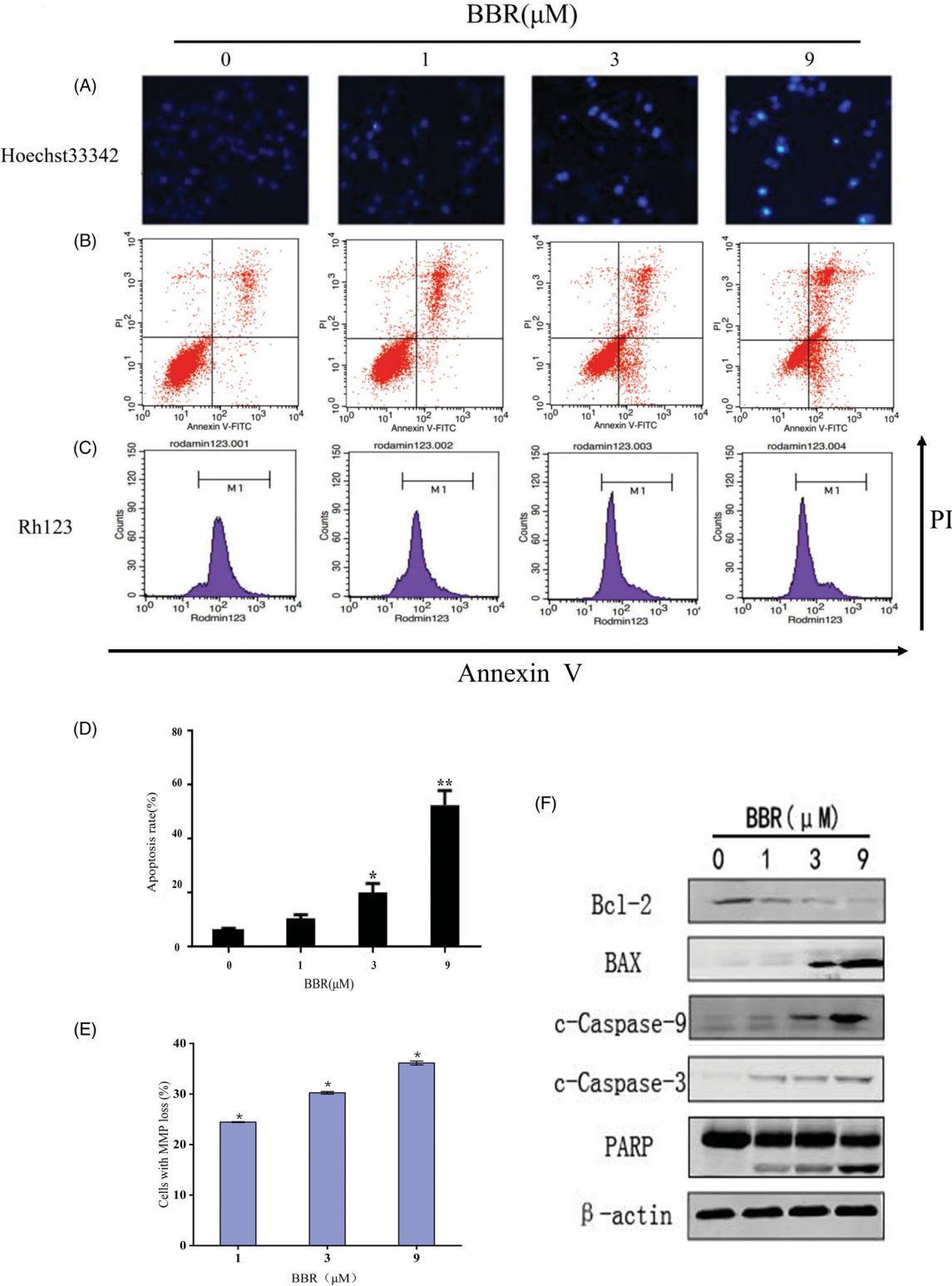


Figure 2. BBR induces cell apoptosis in SW480 cells after 24 h of treatment. (A) Nuclear morphological changes of SW480 cells after 33342 staining. (B) BBR induced apoptosis in SW480 cells. (C) The mitochondrial membrane potential changes of SW480 cells. (D, E) Quantification results of apoptosis and MMP changes in SW480 cells are both expressed as the means \pm S.D. for three independent experiments, $*p < 0.05$, $**p < 0.01$ vs. untreated control. (F) Western blot analysis of Bcl-2, Bax, c-Caspase-9, c-Caspase-3, PARP in BBR treated SW480 cells.

not a HDAC inhibitor as CMAP analysis predicted (Figure 4(D)) (Mariadason 2008). Therefore, although CMAP analysis found that the gene expression profile of BBR is similar to that of Hsp90 and HDAC inhibitors, the direct or indirect interactions between them were not detected.

BBR acted synergistically with Hsp90 and HDAC inhibitors in SW480 cells

In the light of previous study has showed the synergistic effect of BBR with the clinical drug irinotecan (Yu et al. 2014), we tested

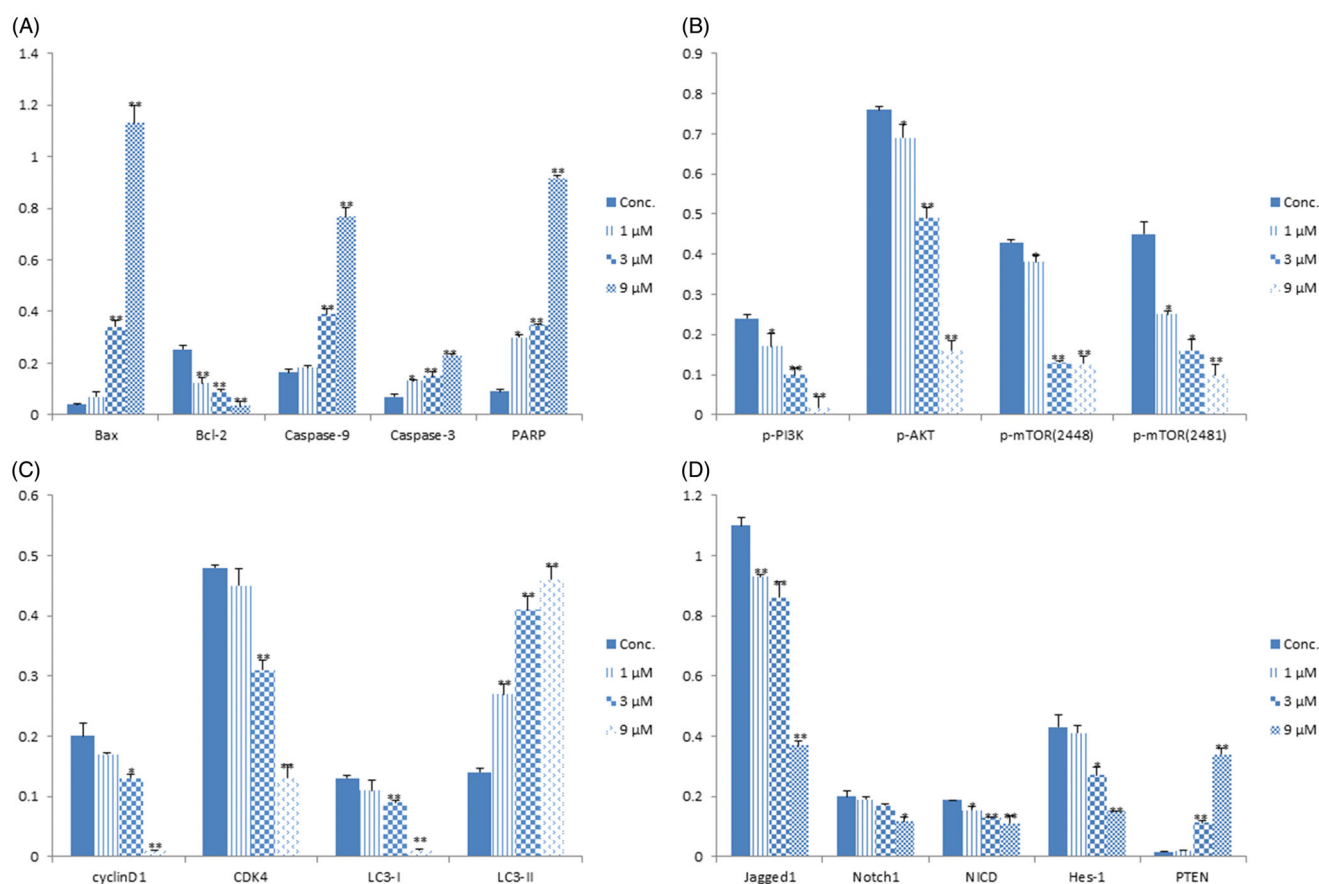


Figure 3. The relative densities of protein bands normalized to β -actin. (A) The relative protein densities of Bax, Bcl-2, Caspase-9, Caspase-3 and PARP. (B) The relative protein densities of p-PI3K, p-AKT, p-mTOR (2448) and p-mTOR (2481). (C) The relative protein densities of cyclinD1, CDK4, LC3-I and LC3-II. (D) The relative protein densities of Jagged1, Notch1, NICD, Hes-1 and PTEN. Data shown are mean \pm standard deviation of three independent experiments. * $p < 0.05$, ** $p < 0.01$ when compared to the control.

Table 2. Expression signatures of CMAP drugs most positively with that of BBR.

| Clinical drugs | Connectivity score | <i>n</i> | <i>p</i> | Specificity | Percent non-null | Function |
|------------------|--------------------|----------|----------|-------------|------------------|------------------------------|
| Helveticoside | 0.517 | 6 | 0 | 0.0085 | 100 | Cardiac stimulant |
| Ianatoside C | 0.471 | 6 | 0 | 0.0092 | 100 | Cardiovascular system agents |
| Pyrvinium | 0.554 | 6 | 0 | 0.0093 | 100 | Antiscolic agents |
| Gossypol | 0.534 | 6 | 0 | 0.0000 | 100 | Contraceptive agents |
| Trifluoperazine | 0.438 | 16 | 0 | 0.0000 | 100 | Dopamine antagonists |
| Geldanamycin | 0.420 | 15 | 0 | 0.0054 | 100 | Hsp90 inhibitor |
| Thioridazine | 0.465 | 20 | 0 | 0.0639 | 100 | Dopamine antagonists |
| Tanespimycin | 0.387 | 62 | 0 | 0.0104 | 95 | Hsp90 inhibitor |
| Prochlorperazine | 0.406 | 16 | 0 | 0.0437 | 93 | Dopamine antagonists |
| Wortmannin | 0.337 | 18 | 0 | 0.0645 | 83 | PI3K inhibitor |
| Sirolimus | 0.318 | 44 | 0 | 0.0301 | 86 | mTOR inhibitor |
| Trichostatin A | 0.217 | 182 | 0 | 0.4123 | 67 | HDAC inhibitor |
| LY-294002 | 0.256 | 61 | 0 | 0.1141 | 75 | PI3K inhibitor |
| Valproic acid | 0.176 | 57 | 0 | 0.0197 | 66 | HDAC inhibitor |

whether BBR has synergistic effects with Hsp90 inhibitor 17-AAG, and HDAC inhibitor SAHA, and whether the combination of the three has synergistic effect. SW480 cells were exposed to 0–20 μ M of 17-AAG, or SAHA, or both 17-AAG and SAHA for 24 h in the presence of 0–2 μ M BBR. CCK-8 assay was applied to determine the cell viability. CompuSyn software was used to calculate the drug combination index (CI). Values of $CI < 1$, $CI = 1$, $CI > 1$ indicate synergistic, superimposed and antagonistic effect, respectively. The smaller the CI value, the more obvious the synergistic effect of the drug is. The results showed that only higher concentrations of BBR (1–2 μ M) show synergistic

effect with SAHA (Figure 5(A,B)). All concentrations of BBR significantly enhanced the anti-proliferative activity of 17-AAG (Figure 5(C,D)), and all of the CI values are less than 1 in Figure 5(E,F) which indicating the combination of BBR, 17-AAG and SAHA has the most potent synergistic effect.

BBR regulates the PI3K/AKT/mTOR pathway and its upstream proteins

The CMAP analysis also revealed that BBR may be a PI3K or mTOR inhibitor. mTOR is the master regulator of cellular

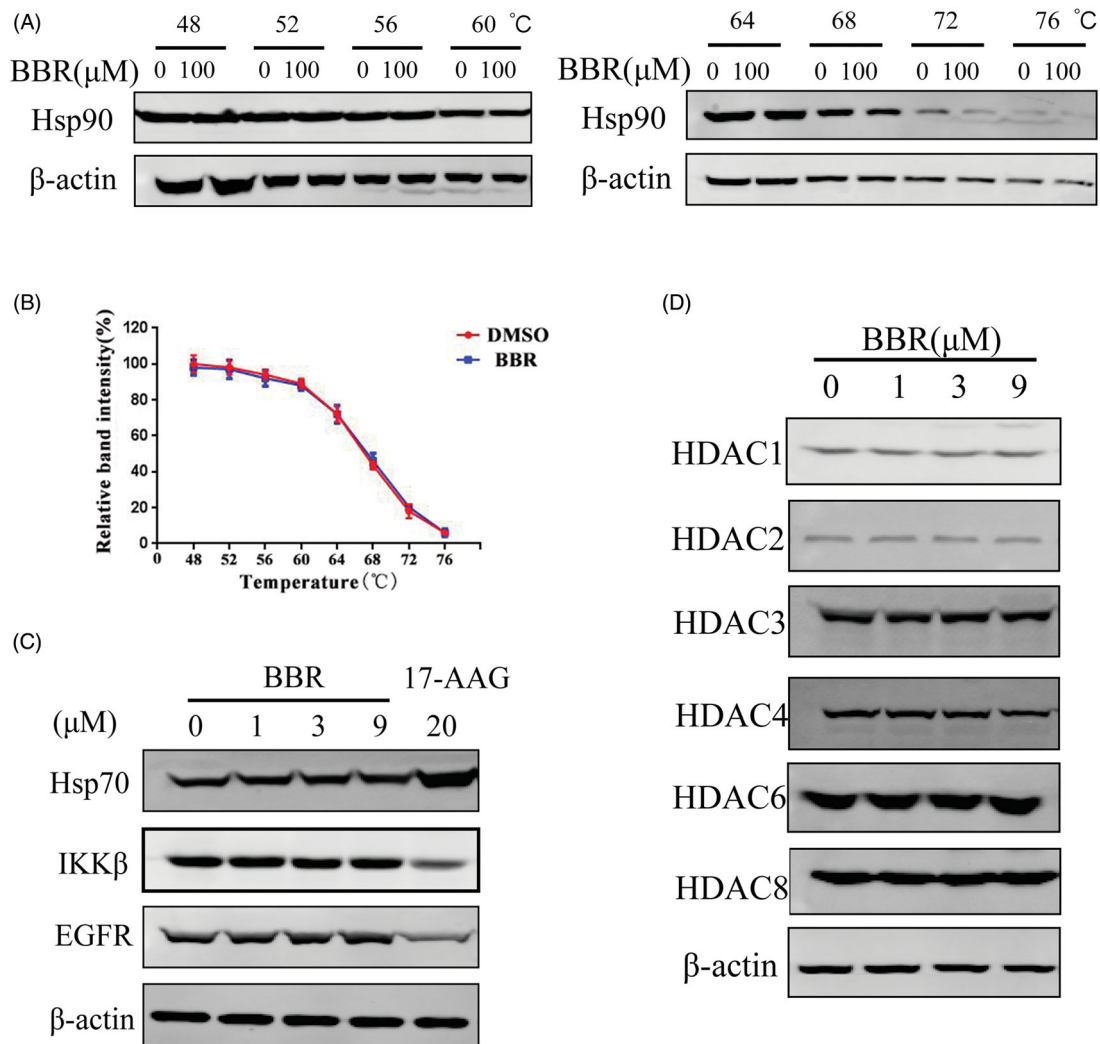


Figure 4. BBR did not inhibit Hsp90 and HDACs in SW480 cells. (A) The binding effect between BBR (100 μ M) and Hsp90 was detected by the thermal stabilization-based CESTA method at 48–76 $^{\circ}$ C after 30 min of incubation at room temperature. (B) Hsp90 protein expression was quantified and the data are presented as means \pm S.D. of three independent experiments. (C) Western blot analysis of Hsp70, IKK β and EGFR in BBR treated SW480 cells after 24 h incubation. The Hsp90 inhibitor 17-AAG was included as positive control. (D) Western blot analysis of HDAC proteins in BBR treated SW480 cells after 24 h incubation.

metabolism, and its deregulation is closely related with cancer. The mTOR was consisted of mTORC1 and mTORC2. PI3K/AKT signalling pathway is the well-established upstream regulator of mTORC1 (Kim and Guan 2015). The decreased levels of p-PI3K, p-Akt and p-mTOR (2448, 2481) in SW480 cells validated the CMAP prediction that BBR is the inhibitor of PI3K/AKT/m-TOR pathway (Figures 3(B) and 6(A)). Inhibition of mTOR phosphorylation can promote autophagy. During autophagy, the cytoplasmic LC3-I enzyme dissolves a small amount of peptides into membrane type LC3-II (Tanida et al. 2008). The ratio of LC3-II/I in SW480 cells increased as the concentrations of BBR increase (Figure 3(C) and 6(D)), indicating that BBR promotes the occurrence of autophagy. In addition, it has been reported that promoting the level of autophagy could augment the arrest of cell cycle, and they are mediated by suppression of PI3K/AKT/m-TOR signalling pathway (Wang et al. 2018). DNA content analysis of SW480 cells showed that BBR induced an increase in the proportion of cells at G1 phase and a decrease at S phase, indicating a G1 phase cell cycle arrest (Figure 6(B)). The observed down-regulations of CyclinD1 and CDK4 in Figures 3(C) and 6(C)) further confirmed the G1 phase arrest of BBR. Therefore, the above studies indicated that BBR inhibits

SW480 cells proliferation by inducing autophagy and cell cycle arrest under the regulation of PI3K/Akt/mTOR pathway.

Notch1 pathway proteins were reported to be highly activated in colon cancer tissues and cells, the inhibition of them may be a promising therapy for colon cancer (Zhang et al. 2010). The activation of Notch1 pathway depends on the interaction of receptors (Notch1, 2, 3, 4) and ligands (Jagged1, 2, DLL1, 3, 4) in adjacent cells. After being cleaved for three times, Notch protein released into the cytoplasm by the intracellular segment (NICD), then NICD entered the nucleus and formed transcriptional activation complex (NICD/CSL), and target proteins (Hes-1, Hes-5, Hey-1, Hey-l) are finally activated (Qiao and Wong 2009). We determined the expression of Notch1, Jagged1, NICD and Hes-1 by Western blot analysis and found that BBR inhibited them in SW480 cells (Figures 3(D) and 6(E)). Thus, BBR can significantly inhibit Notch1 pathway in SW480 cells.

Inhibition of Notch1 pathway could up-regulate the expression of PTEN. PTEN is a well-established tumour-suppressor gene which expressed in all tissues in the body, and its main target is PI3K/AKT/mTOR pathway. Through inhibiting PI3K, AKT and mTOR proteins, PTEN acts as a tumour suppressor by regulating transcription, translation, cell cycle progression,

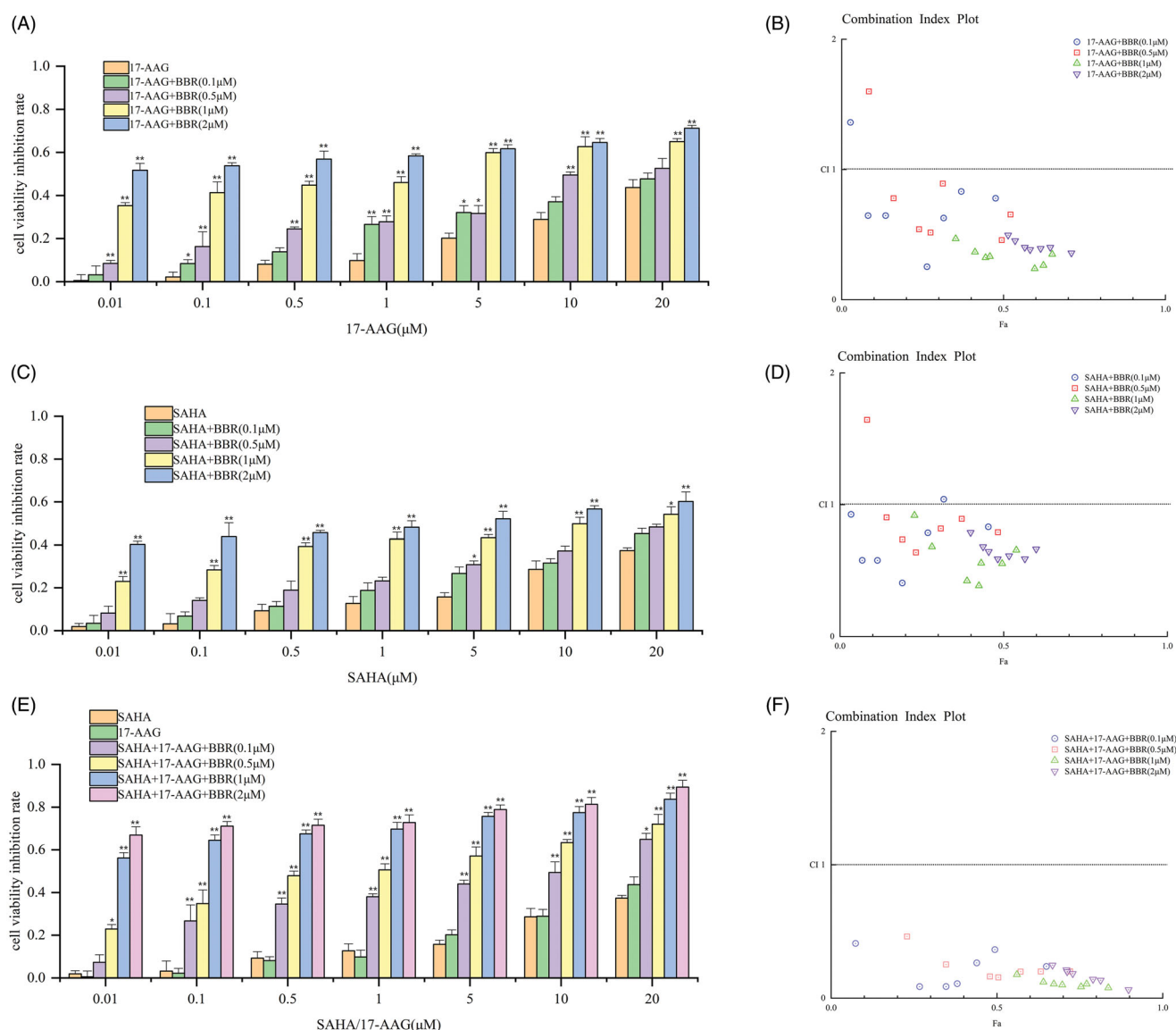


Figure 5. BBR enhanced the anti-proliferative activity of 17-AAG and SAHA, and the combination of the three has more potent synergistic effect on SW480 cells. The incubation time of SW480 cells and the test drugs was 24 h. (A) SW480 cells were exposed to specified concentrations of 17-AAG for 24 h in the presence of 0–2 μM of BBR. (B) The CI values of BBR and 17-AAG combinations. (C) SW480 cells were exposed to specified concentrations of SAHA for 24 h in the presence of 0–2 μM of BBR. (D) The CI values of BBR and SAHA combinations. (E) SW480 cells were treated with specified concentrations of 17-AAG and SAHA in the presence of 0–2 μM of BBR. (F) The CI values for BBR, 17-AAG and SAHA combinations. The above data are all presented as the means \pm S.D. of three independent experiments. * $p < 0.05$, ** $p < 0.01$ when comparing with 17-AAG, SAHA and both 17-AAG and SAHA treatment in the absence of BBR.

angiogenesis and stem cell self-renewal (Lee et al. 2018; Luongo et al. 2019). As observed, PTEN protein in SW480 cells was significantly increased by BBR (Figure 6(E)). Therefore, the inhibition of BBR on Notch1 pathway resulted in the increase of PTEN, following by down-regulation of PI3K/Akt/mTOR pathway, and eventually leading to cell cycle arrest and autophagy in SW480 cells.

Discussion

The natural compound BBR has been long used in Ayurvedic and Chinese medicine for a wide range of pharmacological and biochemical effects. Previous studies indicated that BBR acts on many targets and signal pathways in colon cancer cells; however, systematic understanding of genes and cellular pathways regulated by BBR is needed to define the mechanism of its anticancer action. The CMAP database has been successfully used to

illustrate the mechanisms of many drug candidates and discover new functions of known drugs by analysing the differentially expressed genes and comparing with the FDA approved drugs. The advantage of this chemogenomics-based technique is that it does not focus on single target gene, instead, it focuses on a series of gene expression signatures that used to query the database for similarities with known targets. Our CMAP analysis study found the positive correlations between BBR and Hsp90 inhibitor (17-AAG), HDAC inhibitor (SAHA), PI3K inhibitor and mTOR inhibitor. The interesting finding that BBR act synergistically with 17-AAG and SAHA on SW480 cells, especially the combination of the three has the most potent effect, suggested that BBR is potential to increase the expected maximal antitumor activity of 17-AAG and SAHA alone, and supported exploration of the combination therapy for colon cancer. This study also revealed a novel mechanism for the antitumor activity of BBR through the regulation of Notch1/PTEN/PI3K/AKT/mTOR pathway that

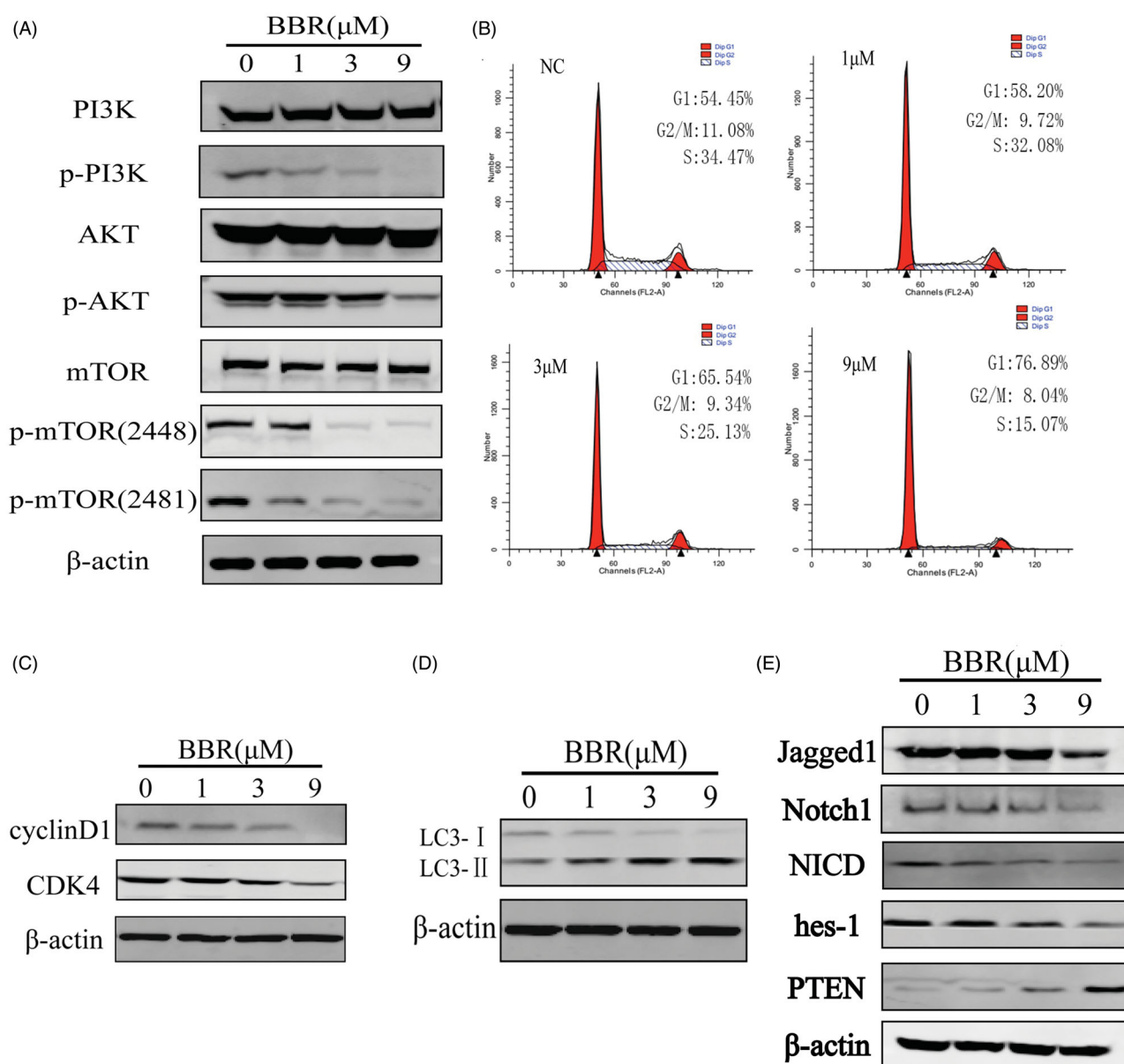


Figure 6. BBR targets the Notch1/PTEN/PI3K/AKT/mTOR pathway, arrests cell cycle and induces autophagy in SW480 cells after 24 h treatment. (A) The total and activated protein levels of PI3K, AKT, mTOR in BBR treated SW480 cells were determined by Western blot. (B) Flow cytometry analysis of cell cycle distribution in BBR treated SW480 cells. (C) Proteins expression of cell cycle related proteins cyclinD1 and CDK4. (D) Proteins expression of autophagy related proteins LC3-I and LC3-II. (E) Proteins expression of Jagged1, Notch1, NICD, hes-1, PTEN and β-actin in BBR treated SW480 cells.

regulates autophagy and cell cycle arrest. In sum, the integrative gene expression profile-based chemical genomics approach in our study provided a useful method to resolve the multi-target mechanisms of BBR. However, considering the use of gene expression profiles from BBR-treated MCF-7 cells which are commonly used in the worldwide laboratories, the variations derived from different cell types should not be neglected. There are also differences between different colon cancer cell lines and experimental conditions. Therefore, more colon cancer cell lines and corresponding non-tumour partners should be employed for mechanistic investigation. The siRNA, protein inhibition, gain-of-function and loss-of-function techniques, and *in vivo* experiments are still needed to clarify the CMAP predictions for BBR. As an improvement and supplement to our CMAP analysis, network pharmacology might help to gain more insights of anticancer mechanism for BBR since it has been successfully used to evaluate many compounds with multiple targets through

the integration of gene expression profiles, metabolomics and protein-protein interactions (Zhao et al. 2019).

Conclusions

Our research provided a new method for studying the anticancer mechanisms of BBR. As CMAP analysis predicted BBR promotes SW480 cells apoptosis, autophagy and cell cycle arrest by inhibiting the PI3K/AKT/mTOR pathway. Further study revealed that BBR can also inhibit and promote the expression of the upstream proteins HDACs and PTEN, respectively. We first found that BBR acts synergistically with Hsp90 and HDAC inhibitors although it does not interact directly with them as CMAP analysis predicted. Our results provide a global view of the mechanisms of action of BBR.

Disclosure statement

The authors declare that we do not have any commercial or associative interest that represents a conflict of interest in connection with the work submitted.

Funding

The work was supported by Grants from Shanghai University of Traditional Chinese Medicine, The 13th College Students' Innovative Activity Project of SHUTCM, and National Science and Technology Major Project of China [2018ZX09731016-005].

References

- Alzamora R, O'Mahony F, Ko WH, Yip TW, Carter D, Irnaten M, Harvey BJ. 2011. Berberine reduces cAMP-induced chloride secretion in T84 human colonic carcinoma cells through inhibition of basolateral KCNQ1 channels. *Front Physiol.* 2:1–10.
- Chidambara Murthy KN, Jayaprakash GK, Patil BS. 2012. The natural alkaloid berberine targets multiple pathways to induce cell death in cultured human colon cancer cells. *Eur J Pharmacol.* 688(1–3):14–21.
- Farooqi AA, Qureshi MZ, Khalid S, Attar R, Martinelli C, Sabitaliyevich UY, Nurmurazayevich SB, Taverna S, Poltronieri P, Xu BJ. 2019. Regulation of cell signaling pathways by berberine in different cancers: searching for missing pieces of an incomplete jig saw puzzle for an effective cancer therapy. *Cancers.* 11(4):478–494.
- Feng Y, Cheung KF, Wang N, Liu P, Nagamatsu T, Tong Y. 2009. Chinese medicines as a resource for liver fibrosis treatment. *Chin Med.* 4:16–26.
- Fukuda K, Hibiya Y, Mutoh M, Koshiji M, Akao S, Fujiwara H. 1999. Inhibition by berberine of cyclooxygenase-2 transcriptional activity in human colon cancer cells. *J Ethnopharmacol.* 66(2):227–233.
- Gao XJ, Wang J, Li MQ, Wang J, Lv J, Zhang L, Sun CF, Ji JM, Yang WB, Zhao ZN, et al. 2019. Berberine attenuates XRCC1-mediated base excision repair and sensitizes breast cancer cells to the chemotherapeutic drugs. *J Cell Mol Med.* 23(10):6797–6804.
- Hieronymus H, Lamb J, Ross KN, Peng XP, Clement C, Rodina A, Nieto M, Du JY, Stegmaier K, Raj SM, et al. 2006. Gene expression signature-based chemical genomic prediction identifies a novel class of HSP90 pathway modulators. *Cancer Cell.* 10(4):321–330.
- Hsu WH, Hsieh YS, Kuo HC, Teng CY, Huang HI, Wang CJ, Yang SF, Liou YS, Kuo WH. 2007. Berberine induces apoptosis in SW620 human colonic carcinoma cells through generation of reactive oxygen species and activation of JNK/p38 MAPK and FasL. *Arch Toxicol.* 81(10):719–728.
- Huang C, Liu H, Gong XL, Wu LY, Wen B. 2017. Effect of evodiamine and berberine on the interaction between DNMTs and target microRNAs during malignant transformation of the colon by TGF- β 1. *Oncol Rep.* 37(3):1637–1645.
- Huang C, Tao L, Wang XL, Pang Z. 2019. Berberine reversed the epithelial–mesenchymal transition of normal colonic epithelial cells induced by SW480 cells through regulating the important components in the TGF- β pathway. *J Cell Physiol.* 234(7):11679–11691.
- Huang C, Wang XL, Qi FF, Pang ZL. 2019. Berberine inhibits epithelial–mesenchymal transition and promotes apoptosis of tumour-associated fibroblast-induced colonic epithelial cells through regulation of TGF- β signalling. *J Cell Commun Signal.* 14(1):53–66.
- Kazaz IO, Mentese A, Demir S, Kerimoglu G, Colak F, Bodur A, Alver A, Kutlu O, Turedi S. 2020. Berberine inhibits the ischemia–reperfusion induced testicular injury through decreasing oxidative stress. *Am J Emerg Med.* 38(1):33–37.
- Kim YC, Guan KL. 2015. mTOR: a pharmacologic target for autophagy regulation. *J Clin Invest.* 125(1):25–32.
- Lamb J, Crawford ED, Peck D, Modell JW, Blat IC, Wrobel MJ, Lerner J, Brunet JP, Subramanian A, Ross KN, et al. 2006. The Connectivity Map: using gene-expression signatures to connect small molecules, genes, and disease. *Science.* 313(5795):1929–1935.
- Lan J, Zhao Y, Dong F, Yan Z, Zheng W, Fan J, Sun G. 2015. Meta-analysis of the effect and safety of berberine in the treatment of type 2 diabetes mellitus, hyperlipemia and hypertension. *J Ethnopharmacol.* 161:69–81.
- Lee YR, Chen M, Pandolfi PP. 2018. The functions and regulation of the PTEN tumour suppressor: new modes and prospects. *Nat Rev Mol Cell Biol.* 19(9):547–562.
- Li W, Hua B, Saud SM, Lin H, Hou W, Matter MS, Jia L, Colburn NH, Young MR. 2015. Berberine regulates AMP-activated protein kinase signaling pathways and inhibits colon tumorigenesis in mice. *Mol Carcinog.* 54(10):1096–1109.
- Lin JG, Chung JG, Wu LT, Chen GW, Chang HL, Wang TF. 1999. Effects of berberine on arylamine *N*-acetyltransferase activity in human colon tumor cells. *Am J Chin Med.* 27(2):265–275.
- Lu L, Hu JL, Wu QP, An Y, Cui W, Wang JW, Ye ZW. 2019. Berberine prevents human nucleus pulposus cells from IL-1 β -induced extracellular matrix degradation and apoptosis by inhibiting the NF- κ B pathway. *Int J Mol Med.* 43(4):1679–1686.
- Lü Y, Han B, Yu H, Cui Z, Li Z, Wang J. 2018. Berberine regulates the microRNA-21-ITGB4-PDCD4 axis and inhibits colon cancer viability. *Oncol Lett.* 15(4):5971–5976.
- Luongo F, Colonna F, Calapà F, Vitale S, Fiori ME, Maria RD. 2019. PTEN tumor-suppressor: the dam of stemness in cancer. *Cancers.* 11(8):1076–1101.
- Lv C, Wu XT, Wang X, Su J, Zeng HW, Zhao J, Shan L, Liu RH, Li HL, Li X, et al. 2017. The gene expression profiles in response to 102 traditional Chinese medicine (TCM) components: a general template for research on TCMs. *Sci Rep.* 7(1):352–361.
- Lv C, Zeng HW, Wang JX, Yuan X, Zhang C, Fang T, Yang PM, Wu T, Zhou YD, Nagle DG, et al. 2018. The antitumor natural product tanshinone IIA inhibits protein kinase C and acts synergistically with 17-AAG. *Cell Death Dis.* 9(2):1–13.
- Ma XL, Chen ZJ, Wang L, Wang GS, Wang ZH, Dong XB, Wen BY, Zhang XC. 2018. The pathogenesis of diabetes mellitus by oxidative stress and inflammation: its inhibition by berberine. *Front Pharmacol.* 9:782–794.
- Mao L, Chen Q, Gong K, Xu X, Xie Y, Zhang W, Cao H, Hu T, Hong X, Zhan YY. 2018. Berberine decelerates glucose metabolism via suppression of mTOR-dependent HIF-1 α protein synthesis in colon cancer cells. *Oncol Rep.* 39(5):2436–2442.
- Mariadason JM. 2008. HDACs and HDAC inhibitors in colon cancer. *Epigenetics.* 3(1):28–37.
- Mohammadijad R, Ahmadi Z, Tavakol S, Ashrafizadeh M. 2019. Berberine as a potential autophagy modulator. *J Cell Physiol.* 234(9):14914–14926.
- Molina DM, Jafari R, Ignatushchenko M, Seki T, Larsson EA, Dan C, Sreekumar L, Cao Y, Nordlund P. 2013. Monitoring drug target engagement in cells and tissues using the cellular thermal shift assay. *Science.* 341(6141):84–87.
- Mondal A, Bennett LL. 2016. Resveratrol enhances the efficacy of sorafenib mediated apoptosis in human breast cancer MCF7 cells through ROS, cell cycle inhibition, caspase 3 and PARP cleavage. *Biomed Pharmacother.* 84:1906–1914.
- Neckers L. 2007. Heat shock protein 90: the cancer chaperone. *J Biosci.* 32(3):517–530.
- Newman DJ, Cragg GM. 2016. Natural products as sources of new drugs from 1981 to 2014. *J Nat Prod.* 79(3):629–661.
- Park JJ, Seo SM, Kim EJ, Lee YJ, Ko YG, Ha J, Lee M. 2012. Berberine inhibits human colon cancer cell migration via AMP-activated protein kinase-mediated downregulation of integrin β 1 signaling. *Biochem Biophys Res Commun.* 426(4):461–467.
- Pirmoradi Z, Yadegari M, Moradi A, Khojasteh F, Mehrjerdi FZ. 2019. Effect of berberine chloride on caspase-3 dependent apoptosis and antioxidant capacity in the hippocampus of the chronic cerebral hypoperfusion rat model. *Iran J Basic Med Sci.* 22(2):154–159.
- Qiao L, Wong BC. 2009. Role of Notch signaling in colorectal cancer. *Carcinogenesis.* 30(12):1979–1986.
- Ruan H, Zhan YY, Hou J, Xu B, Chen B, Tian Y, Wu D, Zhao Y, Zhang Y, Chen X, et al. 2017. Berberine binds RXR α to suppress β -catenin signaling in colon cancer cells. *Oncogene.* 36(50):6906–6918.
- Sahebkar A, Watts GF. 2017. Mode of action of berberine on lipid metabolism: a new-old phytochemical with clinical applications. *Curr Opin Lipidol.* 28(3):282–283.
- Schopf FH, Biebl MM, Buchner J. 2017. The HSP90 chaperone machinery. *Nat Rev Mol Cell Biol.* 18(6):345–360.
- Siegel RL, Miller KD, Jemal A. 2019. Cancer statistics. *CA A Cancer J Clin.* 69(1):7–34.
- Tanida I, Ueno T, Kominami E. 2008. LC3 and autophagy. *Methods Mol Biol.* 445:77–88.
- Tian XH, Yang N, Li B, Zhang JP, Xu XK, Yue RC, Li HL, Chen LP, Shen YH, Zhang WD. 2016. Inhibition of HL-60 cell growth via cell cycle arrest and apoptosis induction by a cycloartane-labdane heterodimer from *Pseudolarix amabilis*. *Org Biomol Chem.* 14(9):2618–2624.
- Wang BJ, Zheng WL, Feng NN, Wang T, Zou H, Gu JH, Yuan Y, Liu XZ, Liu ZP, Bian JC. 2018. The effects of autophagy and PI3K/AKT/m-TOR

- signaling pathway on the cell-cycle arrest of rats primary Sertoli cells induced by zearalenone. *Toxins*. 10(10):398–412.
- Wang LH, Cao HL, Lu N, Liu LP, Wang BM, Hu TH, Israel DA, Peek RM, Polk DB, Yan F. 2013. Berberine inhibits proliferation and down-regulates epidermal growth factor receptor through activation of CBL in colon tumor cells. *PLoS One*. 8(2):e56666.
- Wang LH, Liu LP, Shi Y, Cao HW, Chaturvedi R, Calcutt MW, Hu TH, Ren XB, Wilson KT, Polk DB, et al. 2012. Berberine induces caspase-independent cell death in colon tumor cells through activation of apoptosis-inducing factor. *PLoS One*. 7(5):e36418.
- Wu K, Yang Q, Mu Y, Zhou L, Liu Y, Zhou Q, He B. 2012. Berberine inhibits the proliferation of colon cancer cells by inactivating Wnt/ β -catenin/ β -catenin signaling. *Int J Oncol*. 41(1):292–298.
- Wu YY, Li TM, Zang LQ, Liu B, Wang GX. 2018. Effects of berberine on tumor growth and intestinal permeability in HCT116 tumor-bearing mice using polyamines as targets. *Biomed Pharmacother*. 107: 1447–1453.
- Xu LN, Lu BN, Hu MM, Xu YW, Han X, Qi Y, Peng JY. 2012. Mechanisms involved in the cytotoxic effects of berberine on human colon cancer HCT-8 cells. *Biocell*. 36(3):113–120.
- Xu WS, Parmigiani RB, Marks PA. 2007. Histone deacetylase inhibitors: molecular mechanisms of action. *Oncogene*. 26(37):5541–5552.
- Yao MJ, Fan XD, Yuan B, Takagi N, Liu S, Han X, Ren JG, Liu JX. 2019. Berberine inhibits NLRP3 inflammasome pathway in human triple-negative breast cancer MDA-MB-231 cell. *BMC Complement Altern Med*. 19: 216–227.
- Yu M, Tong X, Qi B, Qu H, Dong S, Yu B, Zhang N, Tang N, Wang L, Zhang C. 2014. Berberine enhances chemosensitivity to irinotecan in colon cancer via inhibition of NF- κ B. *Mol Med Rep*. 9(1):249–254.
- Zhang Y, Li B, Ji ZZ, Zheng PS. 2010. Notch1 regulates the growth of human colon cancers. *Cancer*. 116(22):5207–5218.
- Zhao J, Lv C, Wu QL, Zeng HW, Guo X, Yang J, Tian SS, Zhang WD. 2019. Computational systems pharmacology reveals an antiplatelet and neuro-protective mechanism of Deng-Zhan-Xi-Xin injection in the treatment of ischemic stroke. *Pharmacol Res*. 147:104365–104379.